

RSC Advances



This is an *Accepted Manuscript*, which has been through the Royal Society of Chemistry peer review process and has been accepted for publication.

Accepted Manuscripts are published online shortly after acceptance, before technical editing, formatting and proof reading. Using this free service, authors can make their results available to the community, in citable form, before we publish the edited article. This *Accepted Manuscript* will be replaced by the edited, formatted and paginated article as soon as this is available.

You can find more information about *Accepted Manuscripts* in the [Information for Authors](#).

Please note that technical editing may introduce minor changes to the text and/or graphics, which may alter content. The journal's standard [Terms & Conditions](#) and the [Ethical guidelines](#) still apply. In no event shall the Royal Society of Chemistry be held responsible for any errors or omissions in this *Accepted Manuscript* or any consequences arising from the use of any information it contains.

ARTICLE

Facile synthesis of copper nanoparticle in glycerol at room temperature: Formation mechanism

Cite this: DOI: 10.1039/x0xx00000x

Huei Ruey Ong^{a,b}, Md. Maksudur Rahman Khan^{a*}, Ridzuan Ramli^b, Yonghua Du^c, Shibo Xi^c and Rosli Mohd Yunus^a

Received 00th January 2012,
Accepted 00th January 2012

DOI: 10.1039/x0xx00000x

www.rsc.org/

Copper sol is usually synthesized by the reduction of copper precursor with suitable reducing agent in presence of stabilizer. There are few reports regarding the preparation of copper nanoparticle in glycerol without using stabilizing agent, but at elevated temperature. The formation of reduced copper (Cu⁰) is usually been verified by UV-vis spectrophotometer where a 'red copper sol' was formed. In the present paper we synthesized the copper sol at room temperature in glycerol medium using hydrazine as a reducing agent. The chemical states of copper in the sol and their composition were analyzed by X-ray absorption near edge structure spectroscopy (XANES) with linear composition fitting method. A series-parallel mechanism of the reaction was proposed. An average particle size of 5 ± 1 nm was visualized via transmission electron microscopy (TEM).

Introduction

In recent years copper nanoparticles attracted enormous attention due to catalytic, optical, electrical, antifungal application and low cost¹⁻⁵. Different wet chemical methods have been developed for the synthesis of copper nanoparticles, such as chemical reduction, sol-gel, photochemical, hydrothermal, solvothermal, electrochemical etc^{4, 6-23}. In most of the cases, a stabilizer was used to prevent particle growth and agglomeration. However, the use of strongly bonded protective agents may cause surface deactivation of copper nanoparticles²⁴. Moreover, they can interfere the properties of the nanoparticles in specific applications²⁵. In this context, polyol reduction method has been studied comprehensively as it is an environmental friendly process¹⁰ and polyol plays the role of solvent, mild reducing agent and stabilizer²⁶. The commonly used polyols are ethylene glycol, propylene glycol, diethylene glycol, trimethylene glycol, butylene glycol and glycerol^{27, 28}. The synthesis of copper nanoparticle at high temperatures (135 – 185 °C) in polyols without stabilizer has been reported by Obraztsova, et al.²⁷ and Carroll, et al.²⁸. The average particle size was in the range of 10 – 100 nm. Blossi, et al.²⁹ synthesized copper nanoparticles with a mean diameter of 46 nm using diethylene glycol as the reducing agent and

Polyvinylpyrrolidone (PVP) as the stabilizer at high temperatures (140 – 200 °C). Recently, Kawasaki, et al.²⁴ reported the synthesis of very fine copper nanoparticle (<3 nm) in ethylene glycol without any stabilizing agent at 185 °C. It is a preliminary report and the mechanism of copper formation has not yet been explored. Usually, a high temperature is needed for polyol to start the reduction of the inorganic metal salts and in most cases the size of the resultant particles is in the range of 10 – 100 nm. For low temperature synthesis of copper nanoparticles in polyol, such as glycerol, a strong reducing agent is required. To the best of our knowledge, the synthesis of copper nanoparticles in glycerol at room temperature without using any stabilizer has not been reported previously. Moreover, the formation of copper nanoparticles as a function of time has been undermined throughout the literature. To our understanding, as copper is sensitive towards oxygen/oxygenated compounds, it is very important to identify the various forms of copper during the synthesis of nanoparticles. The goal of this work was to study (i) the formation of copper nanoparticles in glycerol via chemical reduction method at room temperature without a protective agent and its stability at ambient conditions and (ii) the formation of copper sols as a function of time and its mechanism during sol formation.

Experimental section

Materials

Copper(II) chloride salt (CuCl₂•2H₂O), ethanol (99.9%), hydrazine monohydrate (64%), anhydrous glycerol, copper(II) oxide (97%), copper(I) oxide (99.99%), were obtained from

^aFaculty of Chemical & Natural Resources Engineering, Universiti Malaysia Pahang, 26300 Gambang, Pahang, Malaysia.

^bMalaysian Palm Oil Board (MPOB), No. 6, Persiaran Institusi, Bandar baru bangi, 43000 Kajang, Selangor, Malaysia.

^cInstitute of Chemical and Engineering Sciences (ICES), Agency for Science, Technology and Research, 1 Pesek Road, Jurong Island, Singapore 627833.

* E-mail: mrkhancep@yahoo.com

† Electronic Supplementary Information (ESI) available: [details of any supplementary information available should be included here]. See DOI: 10.1039/b000000x/

Sigma-Aldrich (Malaysia) Sdn. Bhd. and used without further purification.

Preparation and characterization of copper sols

The copper nano-sol synthesis was performed in a two-necked round bottom flask (100 mL capacity) with magnetic stirrers at room temperature. The required amount of $\text{CuCl}_2 \cdot 2\text{H}_2\text{O}$ was dissolved in 44 mL glycerol. Subsequently, 6 mL of hydrazine solution was injected drop-wise into the mixture, and the concentration of $\text{CuCl}_2 \cdot 2\text{H}_2\text{O}$ was maintained at 200 mg/L. The hydrazine solution of 7.062 mM was prepared by diluting 64% hydrazine monohydrate with ethanol. The solution was stirred continuously for 14 h. The required amount of samples were withdrawn at different time intervals for analysis. The sample was transferred into a 1 cm optical length quartz cuvette and analysed by UV-Vis (Hitachi U 1800 UV-visible spectrophotometer) and X-ray absorption near edge structure spectroscopy (XANES). For the preparation of 28.6 mg/L sol, the copper precursor (200 mg/L) solution was further diluted with glycerol to the required value and the hydrazine solution (7.062 mM) was diluted with ethanol (99.9%) to 1.01 mM. All other steps were unchanged. The Cu k-edge XANES measurements were conducted at XAFCA facility, Singapore Synchrotron Light Source (SSLS), Singapore. The electron storage ring was operated with an energy of 0.7 GeV (current = 200 – 300 mA). A Si (111) double-crystal monochromator was used for the selection of energy with an energy resolution ($\Delta E/E$) of about 1.9×10^{-4} (eV/eV). The incident photon energy was calibrated using a standard copper foil. In addition, the particle size of final sol was determined by transmission electron microscopy (TEM) (Zeiss Libra 200FE HRTEM operating at 200 kV). The sample for analysis was prepared by placing a drop of the solution prepared by the dilution of as-prepared copper sol with ethanol on a holey perforated carbon film supported on a copper grid, followed by drying at room temperature.

Results and Discussion

Nanoparticle formation

The formation of copper nanoparticles in glycerol was monitored by using UV-Vis spectrophotometer and XANES. The UV-Vis spectrum of the precursor ($\text{CuCl}_2 \cdot 2\text{H}_2\text{O}$) in glycerol before and after the addition of the hydrazine solution, as well as the precursor in aqueous solution, were recorded and presented in Figure 1a. In aqueous solution, Cu^{2+} showed a peak in UV region (at 235 nm) and in visible range it gave a broad and weak absorption band corresponding to the $\text{Cu}(\text{H}_2\text{O})_6^{2+}$ complex³⁰. In glycerol solution, two strong peaks were spotted for the sample before the addition of the reducing agent at 235 and 305 nm. After the addition of hydrazine, the peak at 235 nm was unchanged, but the peak at 305 nm slightly shifted to 310 nm and a closer inspection of the spectrum in the visible range evidenced a shoulder centering at 512 nm (Figure 1a, inset). The characteristic peak at 235 nm can be ascribed by the d-d transition of free Cu^{2+} ³¹. Koyano, et al.³² reported the complex formation in the copper-glycerol solution characterized by two distinct peaks at 392 and 630 nm, where copper sulfate was used as a precursor. In our case, the change of the peak positions might be due to the use of different precursors. The shift of the peak from 305 to 310 nm and the evolution of the shoulder at 512 nm after the addition of hydrazine indicated the formation of Cu^{2+} -glycerol complex. Apart from this, the colour of the solution was changed from light green to light blue after the addition of the reducing agent

suggests the formation of Cu^{2+} -glycerol complex as well, but the UV-Vis data presented in Figure 1 do not confirm it. The formation of the complex in glycerol was further evidenced by XANES. Figure 1b shows the XANES spectra of $\text{CuCl}_2 \cdot 2\text{H}_2\text{O}$ in glycerol, 0 min sample and CuO standard. As shown in Figure 1b, a very weak pre-edge peak appears in all of the three spectra. According to the experimental and theoretical evidence presented by Kosugi, et al.³⁵, this pre-edge peak should be mainly due to the vibronically allowed-dipole 1s-3d transition, which can break the centrosymmetry of the copper site³⁵. The energy position of the pre-edge peak for the three samples is identical and marked as A. The existence of pre-edge peak implies the presence of divalent copper component in the samples. The other main structures for the precursor and 0 min samples are different with respect to both energy position and intensity. These phenomena can be understood in the framework of ligand-to-metal charge transfer (LMCT) and many-electron effects shake down³⁶. Yokoyama, et al.³⁶ presented a detailed study on the structures of XANES of $\text{CuCl}_2 \cdot 2\text{H}_2\text{O}$ crystal based on the comparison of polarized Cu K XANES measurements on oriented single crystals and *ab initio* SCF (self-consistent field) CI (Configuration interaction) calculations. Generally, the peak B_1 for precursor sample and the peak B_2 for 0 min sample can be ascribed to the 1s-4p transition accompanied by the LMCT shake down. The energy position of peak B_1 is much lower than peak B_2 , which indicates that there are two different kinds of LMCT surrounding the absorption atom for precursor and 0 min sample, respectively. In fact, when the reducing agent (hydrazine solution) was added into the precursor solution, the colour changed from light green to light blue immediately. Usually, if Cu^{2+} coordinates with Cl^- , the colour of the compound is light green; and when it coordinates with glycerol, the colour will turn into blue. In this context, before adding the reducing agent into the precursor, Cu^{2+} was bonded with Cl^- , while after addition of reducing agent it was bonded with glycerol. The other evidence was that glycerol would form a complex with Cu^{2+} in alkaline solution, and the reducing agent employed was alkaline^{37, 38}. Thus, we can assign the peak B_1/B_2 as the charge transfer from Cl^- and glycerol, respectively. The structures with energy positions higher than B_1/B_2 , such as C and D, have more complex originations than B_1/B_2 , and each of them can be assigned as the combination of some mechanisms such as: 1s-4p_z or 1s-4p_{x,y} transition with and without CI shake down, 1s-5p_z or 1s-5p_{x,y} with and without LMCT or CI shakedown. Kosugi, et al.³⁵ have studied their detailed origination using *ab initio* calculation. Through comparing the energy positions of those structures, we can find out that the spectrum of the 0 min sample is fairly same as that of the CuO standard. While the spectrum of precursor shows a tendency to move to lower energies relative to that of the 0 min and the CuO standard samples, which can be a result from the stronger LMCT of the precursor that pull down the final state energy of transition.

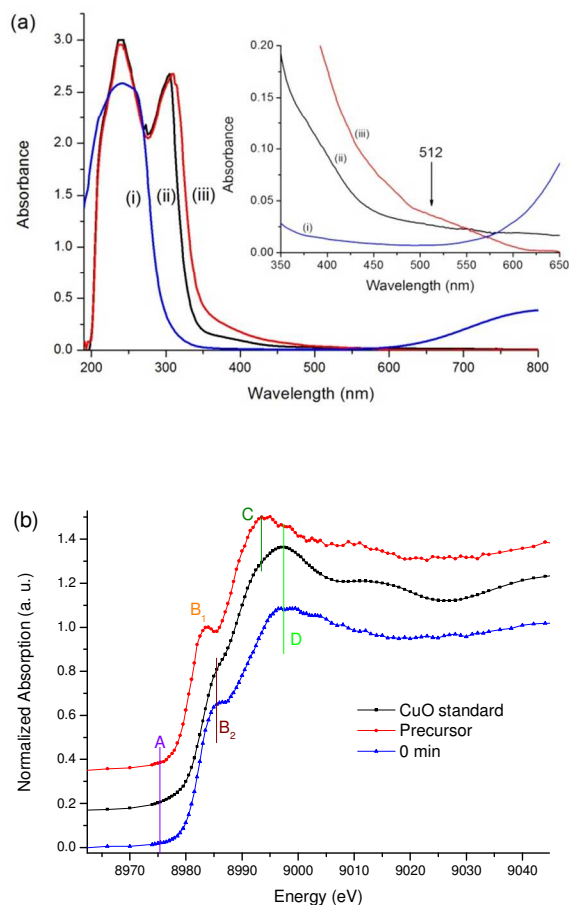


Fig. 1 (a) UV-Vis spectra of CuCl_2 in aqueous solution (i), CuCl_2 in glycerol before (ii), after (iii) addition of hydrazine solution. ($[\text{CuCl}_2] = 28.6$ ppm); (b) XANES spectra of CuO standard, $\text{CuCl}_2 \cdot 2\text{H}_2\text{O}$ in glycerol medium (precursor), 0 min sample (after addition of hydrazine solution). ($[\text{CuCl}_2] = 200$ ppm)

UV-vis spectra of sol formation at different times at 200 ppm of copper are presented in Figure 2a. To capture the spectra in the range of 200 – 400 nm, 28.6 ppm copper sol was prepared and the UV-vis spectra of the sol at different time intervals have been presented in Figure 2a inset. The intensity of both peaks (at 235 and 310 nm) was reduced as the reaction time prolonged. At low copper concentration the colour of the sol changed to pale yellow after 1 h, thereafter the colour turned into light red after 5 h of reaction and retained the same colour until the end of the reaction. With 200 ppm copper solution, after 2 h of reaction, at ~ 530 nm an absorption peak was observed when the sol colour turned into light reddish brown, indicating the presence of Cu^0 . The characteristic Cu^0 plasmon peak at 530 nm was increased as the reaction time increased. The colour of the sol was turned to wine red from light reddish brown after 4 h of reaction. Moreover, after 6 h of reaction the characteristic peak (530 nm) was transformed to two peaks (502 and 560 nm) which indicated that the shape of the particle was changed from spherical to anisotropic^{42,43}. It is well known that, the position and shape of plasmon absorption of

metal nanoparticle are strongly dependent on the particle size, dielectric medium and surface adsorbed species^{44, 45}. According to Mie's theory⁴⁶, a single SPR (surface plasmon resonance) peak was expected for spherical nanoparticles, whereas, anisotropic shape particles could give two or more SPR peaks depending on the shape of the particle. The absorbance of Cu(II) complex (310 nm) and Cu^0 (560 nm) for all reaction time was normalized with respect to the absorbance at 0 h and 9 h respectively and presented in Figure 2b. It can be seen that, the absorbance of Cu(II) complex declined gradually with respect to time. A sharp decrease in the rate of reduction of Cu^{2+} was witnessed after 7 h of reaction. After 10 h of reaction time all Cu(II) complexes had disappeared indicating the completion of the reaction. Meanwhile, a sharp increase in the rate of copper nanoparticle formation was observed after 3 h of reaction and it reached its maximum after 8 h of reaction. The concentration of copper nanoparticle had dropped after 9 h of reaction and the sol colour turned to deep red. This might be due to the formation of CuO . The chemical transformation of Cu^{2+} to Cu^0 appeared to be completed after 9 h of reaction time.

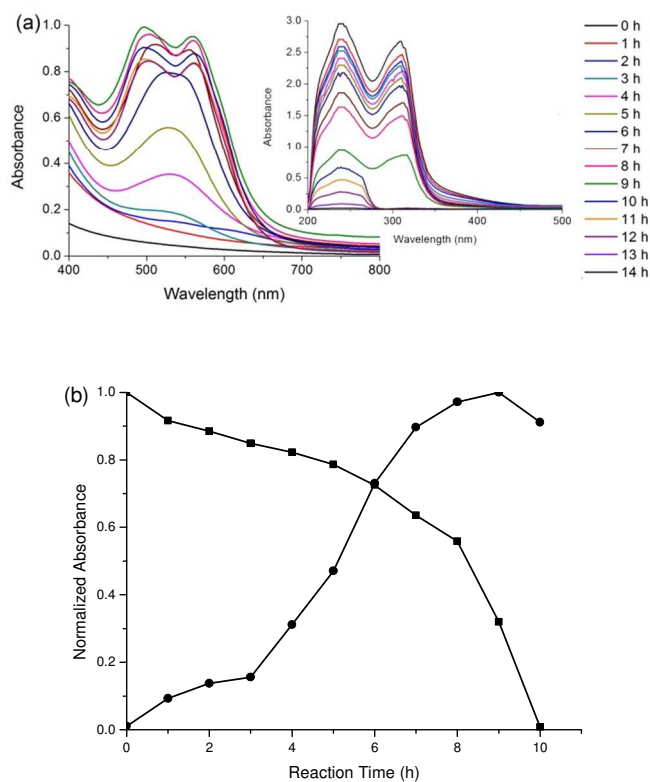


Fig. 2 (a) UV-vis spectra of Cu sol formation, $[\text{CuCl}_2] = 200$ ppm (insert graph: $[\text{CuCl}_2] = 28.6$ ppm); (b) Normalized absorbance of peak at ■ 310 nm and ● 560 nm

Figure 3a illustrates XANES spectra of copper sol formation. The near edge fine structures of Cu^0 were characterized by an absorption resonance at 8981.5 eV,⁴⁷. As shown in Figure 3a, the peak B and peak D shifted towards low energy with reaction time in the first 6 h, and thereafter, shifted towards high energy, which indicated that the copper had been reduced and afterwards re-oxidized. It can be seen that the energy positions of peak B of 6 h sol and Cu standard were quite identical, which demonstrated that the metallic phase copper was formed in sample 6 h. However, the structures around

indicator D of Cu standard sample can not be found in 6 h sol, which implies that the particle size formed is quite small as well as the coexistence of nonmetal phase of copper. As a matter of fact, the surface atom of copper particle can be assumed to be in a nonzero valency state due to the interaction with various ions in the solution, and accompanied with the small particle size; the average valency of copper can be nonzero. The increase of intensity of peak D with reaction time is also an evidence of the formation of copper metallic particle, because the copper crystal has a better degree of order in general than that of Cu^{2+} solution, and the bigger the particle size, the greater the degree of order, the higher resonant peak.

Figure 3b shows the shift of edge of B with reaction time. The shift of the edge represents the reduction of copper. The shift of the edge was very rapid in the first hour and thereafter the rate slightly dropped leading to a maximum at 6 h of reaction. A subsequent decline in shift was observed after 6 h of reaction suggesting the oxidation of Cu^0 . The reaction was taken place under atmospheric environment, so the diffused oxygen from the air might react with the formed Cu^0 . The oxidation and reduction is competing during reaction.

Furthermore, the oxidation state and composition of copper were analysed through the linear composition fitting method^{48, 49} of the XANES data. In order to elucidate the relative composition of the sols, the Cu, Cu_2O and CuO standards were used. The alteration of the Cu(II) complex, Cu^0 , Cu_2O and CuO concentrations during the reaction were shown in Figure 3c. The concentration of Cu(II) complex was reduced throughout the reaction and 100% conversion of precursor was achieved after 10 h. At 1 h of reaction, the concentration of Cu(II) complex, Cu_2O and Cu^0 were 50, 50 and 0%, respectively. This indicates that, Cu^{2+} was initially reduced to Cu^{1+} . Thereafter, the concentration of Cu(II) complex was further decreased to 36% and a sharp increase in Cu^0 concentration (17%) was observed while concentration of Cu_2O was remained almost constant. The result suggests that the reduction of Cu^{2+} to Cu^{1+} and Cu^{1+} to Cu^0 occurred simultaneously. After 4 h of reaction, a significant fall and gain of Cu_2O and CuO concentrations were observed respectively, which corresponded to the oxidation of Cu_2O to CuO. The concentration of Cu^0 was further increased and reached maximum at 6 h (47%) and thereafter Cu^0 and Cu(II) complex concentrations were decreased and reached 17 and 0%, respectively after 10 h of reaction. While, a sharp increase in CuO concentration was perceived and reached 83% after 10 h. This suggests that, Cu^0 was oxidized to CuO. The mechanism of the formation of copper nanoparticles was demonstrated in scheme 1. The copper reduction kinetics analyzed by UV-vis was not in agreement with the XANES results. In most of the reported works, the formation of Cu^0 sol was confirmed by UV-vis spectrophotometer when an absorption peak appeared in the region of 500 – 590 nm and the sol turned into red colour^{4, 10, 29, 50-55}. However, UV-Vis method was unable to identify the state of copper in sol and quantify Cu^0 formation. As shown in UV-Vis spectra, 9 h of reaction is needed to obtain maximum absorbance of Cu^0 whereas, according XANES spectra, 6 h of reaction produced maximum concentration of Cu^0 , but the colour of both samples was red and undistinguishable. From the analysis of XANES spectra, approximately 47% in Cu^0 , 23% in Cu_2O and 26% in CuO for sample at 6 h and 9 h, respectively were found. The XANES result revealed that the red colour sol was a mixture of Cu^0 and CuO, rather than Cu^0 as mentioned in literature^{4, 10, 29, 50-55}. In this context, the optimum reaction time of Cu^0 nanoparticle formation was 6 h.

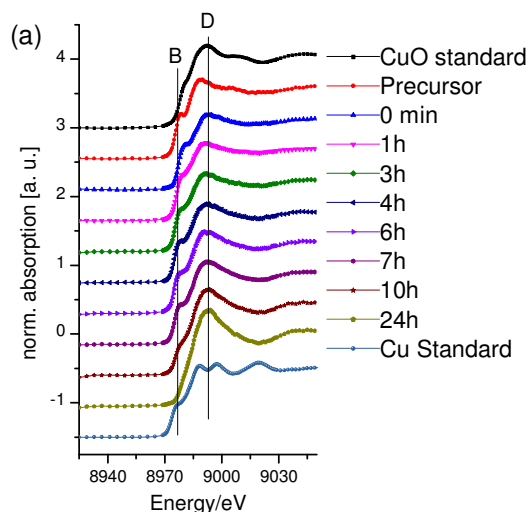


Fig. 3a

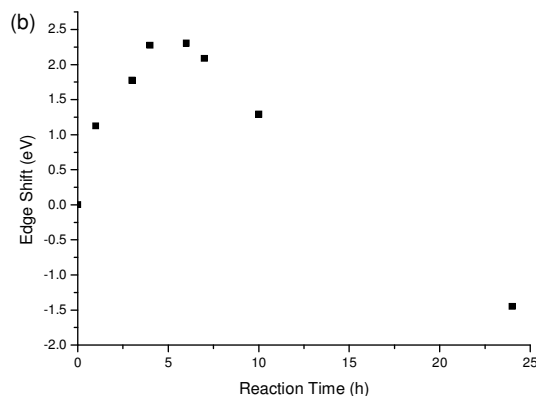


Fig. 3b

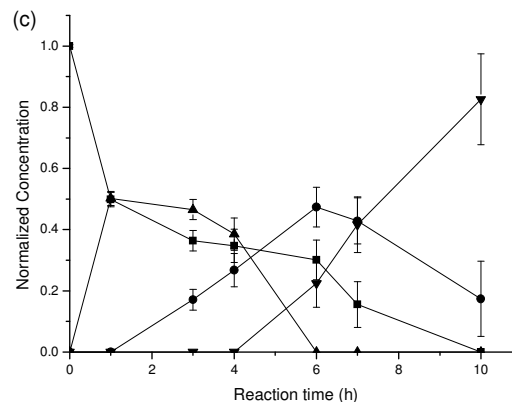
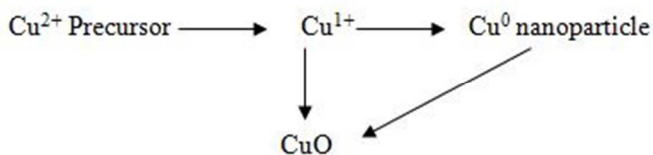


Fig. 3 (a) XANES spectra of copper sol formation ($[\text{CuCl}_2] = 200 \text{ ppm}$); (b) XANES spectra of peak B shift of sol formation with respect to time; (c) Normalized concentration of Cu(II) complex (■), Cu^0 (●), Cu_2O (▲) and CuO (▼) during sol formation.



Scheme 1 Proposed mechanism of copper nanoparticles formation.

TEM of copper nanoparticles

The size of particles of 6 h sol was monitored by TEM and illustrated in Figure 4. TEM image clarifies that the particles developed in the sol are in size of few nanometres. Analyses of 100 – 500 particles of diameters 1.2 – 10.5 nm showed the average particle size of $5 \pm 1 \text{ nm}$. This indicated that, high viscosity of glycerol prevented the agglomeration of the copper nanoparticles⁵⁶.

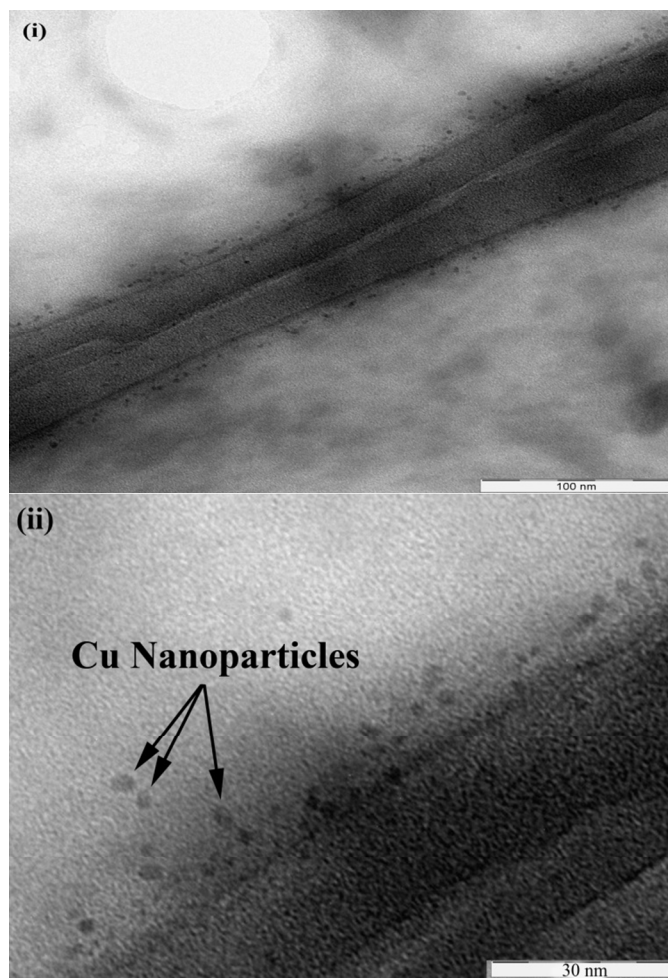


Fig. 4 TEM micrograph of copper nanoparticles at low magnification (i), high magnification (ii).

Conclusions

We proposed a simple low-temperature chemical reduction method for the synthesis of copper nanoparticle in glycerol without using the stabilizer. The mechanism of the sol formation has been demonstrated. In addition, we confirmed the composition of the sol as a function of time. When the sol was prepared in oxygenated solvent, copper oxide formation was inevitable, therefore the colour appearance of the sol cannot be used to determine Cu^0 formation. Hence, the composition of the sol is very important in specific applications.

Acknowledgements

This work was financially supported by research grant from Universiti Malaysia Pahang, Malaysia (Project No: RDU140322 and GRS 130350) and GSAS scholarship (Huei Ruy Ong) from Malaysian Palm Oil Board for which the authors are very grateful.

Notes and references

1. M. N. K. Chowdhury, M. D. H. Beg, M. R. Khan and M. F. Mina, *Mater. Lett.*, 2013, 98, 26-29.
2. Z. Huang, F. Cui, H. Kang, J. Chen, X. Zhang and C. Xia, *Chem. Mater.*, 2008, 20, 5090-5099.
3. A. A. Ponce and K. J. Klabunde, *J. Mol. Catal. A: Chem.*, 2005, 225, 1-6.
4. C. Dong, H. Cai, X. Zhang and C. Cao, *Physica E: Low-dimensional Systems and Nanostructures*, 2014, 57, 12-20.
5. R. Kaur, C. Giordano, M. Gradzielski and S. K. Mehta, *Chemistry—An Asian Journal*, 2014, 9, 189-198.
6. N. A. Dhas, C. P. Raj and A. Gedanken, *Chem. Mater.*, 1998, 10, 1446-1452.
7. Z. Liu and Y. Bando, *Adv. Mater.*, 2003, 15, 303-305.
8. M. Yang and J.-J. Zhu, *J. Cryst. Growth*, 2003, 256, 134-138.
9. M.-S. Yeh, Y.-S. Yang, Y.-P. Lee, H.-F. Lee, Y.-H. Yeh and C.-S. Yeh, *J. Phys. Chem. B*, 1999, 103, 6851-6857.
10. Y. Zhao, J. J. Zhu, J. M. Hong, N. Bian and H. Y. Chen, *Eur. J. Inorg. Chem.*, 2004, 2004, 4072-4080.
11. H. Wang, J.-Z. Xu, J.-J. Zhu and H.-Y. Chen, *J. Cryst. Growth*, 2002, 244, 88-94.
12. R. V. Kumar, Y. Diamant and A. Gedanken, *Chem. Mater.*, 2000, 12, 2301-2305.
13. R. V. Kumar, Y. Mastai, Y. Diamant and A. Gedanken, *J. Mater. Chem.*, 2001, 11, 1209-1213.
14. G. G. Condorelli, L. L. Costanzo, I. L. Fragalà, S. Giuffrida and G. Ventimiglia, *J. Mater. Chem.*, 2003, 13, 2409-2411.
15. S. Kapoor and T. Mukherjee, *Chem. Phys. Lett.*, 2003, 370, 83-87.
16. A. V. Loginov, V. V. Gorbunova and T. B. Boitsova, *J. Nanoparticle Res.*, 2002, 4, 193-205.
17. Z. Liu, Y. Yang, J. Liang, Z. Hu, S. Li, S. Peng and Y. Qian, *J. Phys. Chem. B*, 2003, 107, 12658-12661.
18. S.-J. Chen, X.-T. Chen, Z. Xue, L.-H. Li and X.-Z. You, *J. Cryst. Growth*, 2002, 246, 169-175.
19. E. W. Bohannon, M. G. Shumsky and J. A. Switzer, *Chem. Mater.*, 1999, 11, 2289-2291.
20. J. K. Barton, A. A. Vertegel, E. W. Bohannon and J. A. Switzer, *Chem. Mater.*, 2001, 13, 952-959.
21. L. Huang, H. Wang, Z. Wang, A. Mitra, D. Zhao and Y. Yan, *Chem. Mater.*, 2002, 14, 876-880.
22. W. Wang, Y. Zhan and G. Wang, *Chem. Commun.*, 2001, 727-728.
23. R. Sierra-Ávila, M. Pérez-Alvarez, G. Cadenas-Pliego, C. A. Ávila-Orta, R. Betancourt-Galindo, E. Jiménez-Regalado, R. M. Jiménez-Barrera and J. G. Martínez-Colunga, *Journal of Nanomaterials*, 2014, 2014, 361791.
24. H. Kawasaki, Y. Kosaka, Y. Myoujin, T. Narushima, T. Yonezawa and R. Arakawa, *Chem. Commun.*, 2011, 47, 7740-7742.
25. M. R. Khan and S. D. Lin, *J. Power Sources*, 2006, 162, 186-191.
26. C. Feldmann and H. O. Jungk, *Angew. Chem. Int. Edit.*, 2001, 40, 359-362.

27. I. I. Obraztsova, G. Y. Simenyuk and N. K. Eremenko, *Russ. J. Appl. Chem.*, 2009, 82, 981-985.
28. K. J. Carroll, J. U. Reveles, M. D. Shultz, S. N. Khanna and E. E. Carpenter, *J. Phys. Chem. C*, 2011, 115, 2656-2664.
29. M. Blosi, S. Albonetti, M. Dondi, C. Martelli and G. Baldi, *J. Nanoparticle Res.*, 2011, 13, 127-138.
30. T. Lister, *Modern chemical techniques*, Royal Society of Chemistry, 1995.
31. A. J. Pardey, A. D. Rojas, J. E. Yáñez, P. Betancourt, C. Scott, C. Urbina, D. Moronta and C. Longo, *Polyhedron*, 2005, 24, 511-519.
32. H. Koyano, M. Kato and H. Takenouchi, *Journal of the Electrochemical Society*, 1992, 139, 3112-3116.
33. J. Rothe, J. Hormes, H. Bönemann, W. Brijoux and K. Siepen, *J. Am. Chem. Soc.*, 1998, 120, 6019-6023.
34. Y. Song, E. E. Doomes, J. Prindle, R. Tittsworth, J. Hormes and C. S. S. R. Kumar, *J. Phys. Chem. B*, 2005, 109, 9330-9338.
35. N. Kosugi, T. Yokoyama, K. Asakura and H. Kuroda, *Chem. Phys.*, 1984, 91, 249-256.
36. T. Yokoyama, N. Kosugi and H. Kuroda, *Chem. Phys.*, 1986, 103, 101-109.
37. A. H. Hazimah, M. Badri, K. A. Crouse and A. R. Manas, *Palm Oil Developments*, 2001, 35, 8-10.
38. K. F. Pirker, M. C. Baratto, R. Basosi and B. A. Goodman, *J. Inorg. Biochem.*, 2012, 112, 10-16.
39. J. Kim, S. W. Kang, S. H. Mun and Y. S. Kang, *Ind. Eng. Chem. Res.*, 2009, 48, 7437-7441.
40. H. R. Ong, M. R. Khan, M. N. K. Chowdhury, A. Yousuf and C. K. Cheng, *Fuel*, 2014, 120, 195-201.
41. H. R. Ong, M. R. Khan, R. Ramli and R. M. Yunus, *Appl. Mech. Mater.*, 2014, 481, 21-26.
42. S. Pal, Y. K. Tak and J. M. Song, *Appl. Env. Microb.*, 2007, 73, 1712-1720.
43. C. Noguez, *J. Phys. Chem. C*, 2007, 111, 3806-3819.
44. U. Kreibitz and M. Vollmer, *Optical properties of metal clusters*, Springer Berlin Heidelberg, 1995.
45. P. Mulvaney, *Langmuir*, 1996, 12, 788-800.
46. G. Mie, *Ann. Phys.*, 1908, 25, 377-445.
47. T. Li Hsiung, H. P. Wang, Y.-M. Lu and M.-C. Hsiao, *Radiation Physics and Chemistry*, 2006, 75, 2054-2057.
48. C.-Y. Liao, H. P. Wang, F.-L. Chen, C.-H. Huang and Y. Fukushima, *Journal of Nanomaterials*, 2009, 2009, 698501.
49. S.-H. Liu, H. P. Wang, C.-H. Huang and T.-L. Hsiung, *Journal of synchrotron radiation*, 2010, 17, 202-206.
50. J. Xiong, Y. Wang, Q. Xue and X. Wu, *Green Chem.*, 2011, 13, 900-904.
51. J. L. C. Huaman, K. Sato, S. Kurita, T. Matsumoto and B. Jeyadevan, *J. Mater. Chem.*, 2011, 21, 7062-7069.
52. X. Zhu, B. Wang, F. Shi and J. Nie, *Langmuir*, 2012, 28, 14461-14469.
53. D. Deng, Y. Jin, Y. Cheng, T. Qi and F. Xiao, *ACS applied materials & interfaces*, 2013, 5, 3839-3846.
54. D. Zhang and H. Yang, *Phys. B: Condens. Matter.*, 2013, 415, 44-48.
55. S. Yallappa, J. Manjanna, M. A. Sindhe, N. D. Satyanarayan, S. N. Pramod and K. Nagaraja, *Spectrochim. Act. Part A: Mol. Biomol. Spec.*, 2013, 110, 108-115.
56. K. Patel, S. Kapoor, D. P. Dave and T. Mukherjee, *J. Chem. Sci.*, 2005, 117, 53-60.